

Estimation of Soil Moisture and Biomass Changes Using SAR Data During MEDA-Spain Experiment*

S.S. Saatchi, J. Van Zyl, and D. Evans**

Jet Propulsion Laboratory
California Institute of Technology
4800 Oak Grove Drive
Pasadena, California 91109

ABSTRACT

During the 1991 MAC-EUROPE campaign, the Castilla-La-Mancha region of Spain was surveyed by the multi-frequency (L-, S-, C-band) polarimetric AIRSAR of Jet Propulsion Laboratory. The experiment was devised to demonstrate the role of SAR imagery in detecting and estimating surface parameters such as soil moisture and canopy water content. Two SAR images which were acquired almost a month apart (June 19 and July 14, 1991) over Barrax site have been analyzed in conjunction with ground truth data in order to show the sensitivity of SAR frequency and polarization combinations to variations of surface parameters. It is shown that the L-band and C-band HH polarizations are more suitable to estimate the canopy water content whereas HH and VV polarizations are sensitive to both canopy water content and soil surface moisture. Thus, an inversion algorithm based on cross-polarized properties of SAR data has been developed to estimate the canopy water content. The results of the inversion technique is in agreement with ground truth measurements and site observations. The canopy water content is then used to correct the co-polarized backscattered images for vegetation effects and new images are created which are only sensitive to soil surface moisture and roughness. From the new images, the surface soil moisture over the entire region is estimated and the result is compared with in situ measurements.

1.0 INTRODUCTION

The measurement of soil moisture is important for understanding the global hydrologic cycle and its effect on weather and climate. On a global scale, soil moisture is important as a boundary condition for hydrologic and climate models. On a regional scale, it is important for agricultural assessment (crop yield models, drought assessment, etc) and flood control. Microwave sensors offer the potential for remotely measuring moisture in the soil because of the large change the addition of water makes to the dielectric constant of

* Presented at the 25th International Symposium, Remote Sensing and Global Environmental Change., Graz, Austria, 4-8 April 1993.

** This work was performed at the Jet Propulsion Laboratory, California Institute of Technology supported by the National Aeronautics and Space Administration.

dry soil [Pingman and Gurney, 1991]. However, the presence of a vegetation canopy complicates the retrieval of moisture in the underlying soil because the canopy scatters and contains moisture of its own.

In recent years, there has been an intensive effort among remote sensing scientists to understand the effect of vegetation in retrieving soil moisture and to develop techniques to monitor and measure the vegetation biophysical status on regional and global scales. These efforts are mainly centered around 1) the parametrization of the vegetation canopies such as forest, grasslands, and agricultural crops, 2) the development of sensors, both optical and microwave, for monitoring and measuring land-surface parameters, and 3) the development of algorithms to estimate surface parameters over a variety of environmental conditions and spatial scales. One of the most useful parameters for defining the vegetation status is the canopy water content and/or biomass. Microwave instruments are shown to be sensitive to canopy water content in particular in agricultural fields and natural pastures. By knowing the canopy water content, one might be able to eliminate the shielding effect of vegetation and to estimate the soil moisture over a variety of land surfaces.

In this study, estimation of soil moisture and canopy water content of agricultural crops are considered. These canopies are often considered sparse or low vegetated. Due to the penetration of radar transmitted signal through crop canopies, the water content of the canopy and the moisture of underlying soil affect the received signal [Ulaby, *et al.*, 1986]. For dense canopies such as forests, the radar received signal is sensitive to the water content of the top layer of the canopy. Recently, there have been studies to relate the radar return signal to the forest biomass and possibly infer valuable information about the forest stands [LeToan, *et al.*, 1992, Dobson, *et al.*, 1992].

This study is focused on the data acquired during the MAC-EUROPE campaign during the summer of 1991. The objectives of the experiment are discussed elsewhere [Bolle and Streckenbach, 1992]. The Jet Propulsion Laboratory team acquired images over the Castilla-La-Mancha area using the SAR (Synthetic Aperture Radar) aboard the NASA DC-8 aircraft. The SAR data have the potential to contribute to the experiment goals by measuring surface parameters, in particular, for scaling estimated soil moisture and vegetation parameters from high resolution (meters) to local (km) and regional scales (10-100 km), SAR may play a significant role [Saatchi *et al.*, 1993].

The experiment site is discussed in section 2.0. In section 3.0, the SAR data acquired over Barrax are explained and the processing and calibration procedures are discussed. In section 4.0, a synoptic review of the *in situ* measurements during the SAR flights are given. The modeling and inversion algorithms are discussed in sections 5.0 and 6.0 respectively. A summary and the concluding remarks are given in section 7.0.

2.0 Study Area

The experimental sites during the MEDA (European International Program on Climate Hydrological Interactions between Vegetation, Atmosphere, and Land Surface, ICHVAL, Field Experiment in Desertification Threatened Areas) campaign covered an area of almost 10^4 km^2 between $38^\circ 55' - 40^\circ 05' \text{ N}$ and $2^\circ 11' - 3^\circ 11' \text{ W}$ in the central plateau of Spain within the Castilla-La-Mancha basin. Three supersites within the experimental area were chosen for the field activities and aircraft measurements. The area is a relatively flat plain bounded by mountains to the north, east and south. Due to the overexploitation of groundwater resources for crop irrigation, there has been a continuous

depletion of the groundwater elevation. It has been shown that this area, compared to its neighboring basins with less dramatic decrease in groundwater, will severely contribute to climate changes and may cause higher mean temperatures and lower rainfalls [Bolle and Streckenbach, 1992].

From the three supersites only the Barrax site is chosen for the SAR data analysis in this study. This site is situated in the west of the province of Albacete, 28 km from the Capital town. The landscape is flat with no change of elevation more than 2% (slopes less than 2 m) over the whole area. The regional water table is 20-30 m below the land surface.

The climate of the area is Mediterranean, with heaviest rainfalls in spring and autumn and lowest in summer. The average annual temperature is 14.1°C, the hottest month is July with average temperature of 24.6°C and the coldest month is January with an average temperature of 3.90°C. The average rainfall in the region is 500 mm with 72 rainy days and the evapotranspiration is 775 mm [Visser and Hoakman, 1992].

The surface area of the site is approximately 10,000 ha which is dominated by dry land and irrigated land cultivations distributed as given in Table 1.

Table 1 Distribution of the land cover in Barrax site

Dry Land and Cultivation	Irrigated land
6514 ha (65%):	3486 (35%)
Winter Cereals 67%	Corn 75%
Fallow land 33%	Barley-Sunflower 15%
	Alfalfa 5%
	Onions 3%
	Vegetables 2%

Figure 1 shows the land cover distribution in the Barrax site. During the experiment the land use and the crop covers do not completely match with the ones shown in Figure 1. In the beginning of June majority of the fields were not cultivated or had very low vegetation cover. Whereas in July the crop canopies were at later growth stage and had considerable vegetation cover. In SAR data analysis, we will focus on the fields where the vegetation cover changes during the time between the two experiments.

3.0 SAR DATA

SAR data were acquired over all three supersites on June 19 and July 14, 1991. The sensor parameters are given in Table 2. In the JPL AIRSAR system the received wave is decomposed into two orthogonal polarized components, which independently feed two identical and coherent received channels. The reception polarization diversity is accomplished by transmission polarization diversity so that an object's complete scattering matrix can be measured [Van Zyl, *et al.*, 1987, Evans, *et al.*, 1988]. The basic datum measured by AIRSAR is, therefore, a complex (amplitude and phase) scattering matrix for each resolution cell. For reasons of reducing the data, the Stokes matrix is calculated from the measured scattering matrix and stored in a compressed format. The three-frequency compressed images are approximately 12.5 Mbyte. Each pixel contains 10 bytes of data which corresponds to 9 independent elements of a symmetric observed Stokes matrix.

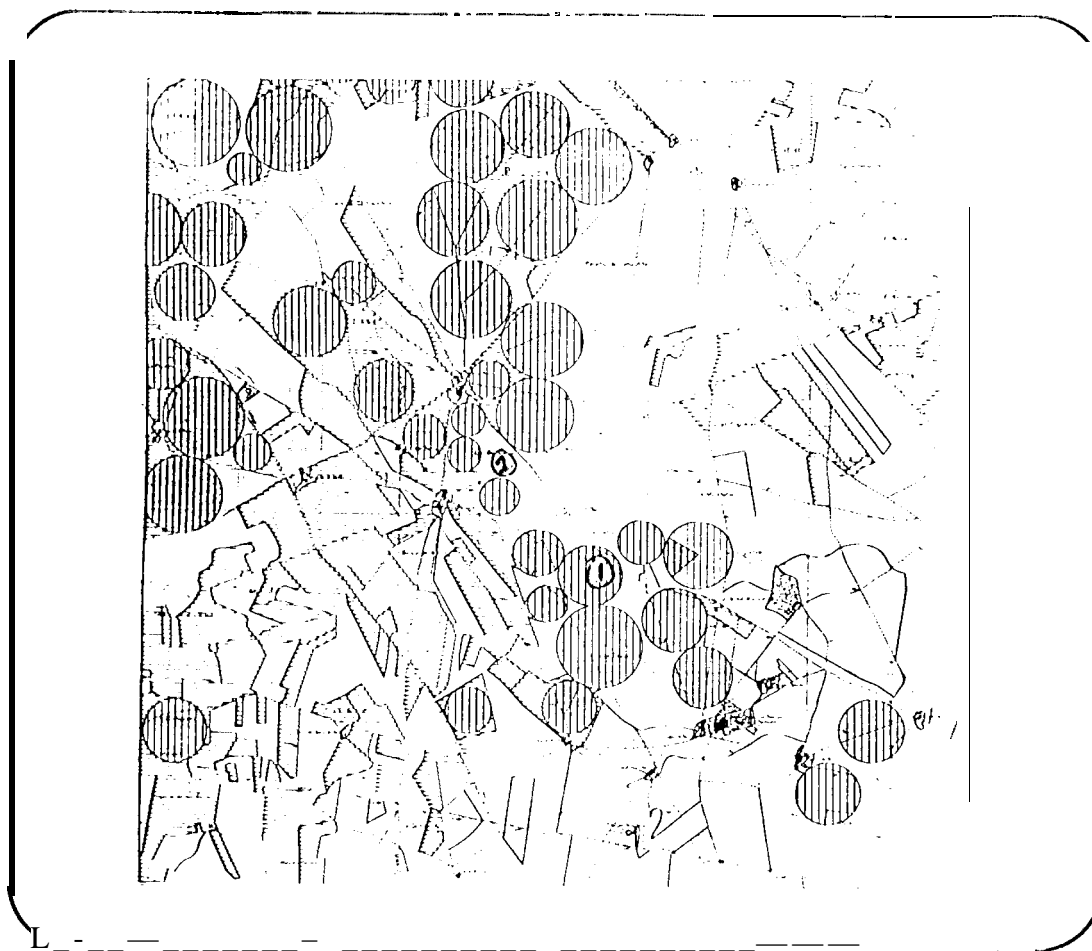


Figure 1. The land cover distribution in the Barrax site,

The processing technique utilized to process the AIRSAR data produces images of 16 look average of an area of 12. km x 8.5 km with a pixel spacing of 6 m and 12 m in slant range and azimuth respectively. The SAR images are provided in a compressed format at three frequencies to the user. Two types of complimentary calibration procedures are used, 1) internal calibration, and 2) external calibration. For the internal calibration, the information collected from the system tests which are performed regularly during a flight campaign are used to obtain calibration parameters to be used in the AIRSAR processor. This will ensure that all the 4 channels (4 polarizations) are calibrated relative to one another at each frequency [Van Zyl, 1992].

External calibration allows absolute calibration of the radar cross section of the scene including the removal of the cross talk and the channel imbalance. To do this, we use the information from the scene and trihedral corner reflectors as external targets. The responses from the corner reflectors are analyzed to calculate the absolute calibration parameters. The absolute calibration parameters are then provided to the AIRSAR processor in order to produce calibrated images. In addition, corner reflectors were deployed on the ERTDA sites (4 corner reflectors at the Barrax site) during the experiment which are used to check the accuracy of the AIRSAR calibration.

Table 2. Characteristics of the J[']. AIRSAR multi-polarization and multi-frequency system.

Frequencies (P-, L-, C-band):	0.44, 1.23, 5.3 GHz
Polarizations:	HH, HV, VV, VV
Swath Width:	8.5 km
Incidence Angle Across Swath:	15° - 60°
Range Pixel Size:	6 m
Azimuth Pixel Size:	12 m
No. of Range Samples:	1280
No. of Azimuth Samples:	1024
Nominal Altitude:	8 km
Platform:	NASA DC-8

4.0 Field Measurements

Analysis of the SAR data and the verification of the SAR derived surface parameters depend on the availability of the ground truth data. During the SAR flights, ground truth data were collected over selected fields and plots at the Barrax site (Figure 1). The measurements were conducted by many investigators during the first SAR flight. In this study, we use the soil moisture and roughness measurements collected by the Wageningen Agricultural University in The Netherlands over the Barrax site [Visser and Hockman, 1992]. The vegetation sampling were conducted by the University of Albacete, Spain. During the second day of the AIRSAR flights, soil moisture and vegetation structural measurements were conducted by the J['] group over limited fields [Saatchi *et al.*, 1993].

The soil water content were measured by gravimetric soil sampling and the neutron probe measurements. In addition, volumetric soil moisture sampling were carried out in the surface layers of 0-5 cm and 5-10 cm depths. At certain selected fields, the time evolution of soil moisture at various depths and moisture depth profile were also measured [Bolle and Streckenbach, 1992]. The results indicate that the soil moisture variations occur within the first 50 cm depth from the surface and the hydraulic head stays almost constant at the depth of 70 cm. The irrigation of the fields has caused a sharp increase of water content at the depths of 10 and 20 cm. In the analysis of the SAR data, we are only interested in soil moisture of the top 10 cm where the radar signal can penetrate. This layer is also known to be an active layer for the evaporation process during the summer months in this climate region. The ground truth data given in Table 3 are used to verify SAR derived parameters in the following sections.

Table 3. Field measurements over two fields at the Barrax site [Saatchi, 1992, Bolle and Streckenbach, 1992, Visser and Hockman, 1992].

Field	Crop	Biomass 6/19/91	Biomass 7/14/91	soil moisture 6/19/91	soil moisture 7/14/91	RMS Height
1	Corn	1.6 kg/m ²	4.1 kg/m ²	0.18 g/cm ³	-	1.12 cm
2	Bare	0	0	0.03 g/cm ³	0.04 g/cm ³	1.65 cm

5.() Scattering Model

The backscattering model used in this study is based on the Distorted Born Approximation (DBA) [Lang and Sidhu, 1983]. We have simplified the DBA model in order to retrieve the soil and vegetation parameters directly. The electromagnetic scattering model for a general vegetation canopy is shown in Figure 2. "Here, a vegetation canopy of thickness d over a lossy rough ground surface having complex dielectric constant ϵ is shown. The canopy is modeled as an ensemble of leaves and branches. The leaves are elliptical dielectric discs and the branches are dielectric circular cylinders which are distributed uniformly in the azimuth direction. This model has been applied to corn and soybean canopies where the parameters such as size, orientation distributions and dielectric constant of the vegetation components have been used as inputs to the model [Saatchi, 1992.] .

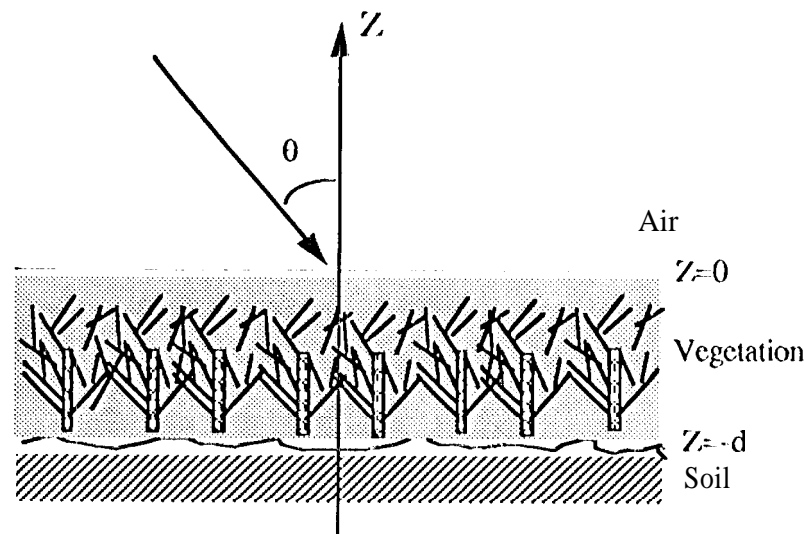


Figure 2. Vegetation Canopy Model

The common approach to model the electromagnetic scattering from a canopy consists of two steps, 1) to relate the SAR measured backscattering coefficients to the scene and 2) to relate the model parameters to the physical parameters of the canopy. The backscattering coefficients measured by SAR can be decomposed into vegetation and soil contributions.

$$\sigma_{\text{canopy}}^0 = \sigma_{\text{veg}}^0 + \sigma_{\text{soil}}^0 \quad (1)$$

According to the DBA model one can further decompose the vegetation contribution to several scattering mechanisms from which only the volume scattering and the surface-volume interaction terms are dominant. Therefore, the vegetation component can be written as:

$$\sigma_{\text{veg}}^0 = \sigma_{\text{vol}}^0 + \sigma_{\text{vol-soil}}^0 \quad (2)$$

Depending on the type of the vegetation canopy the weight of each term in the total vegetation contribution may vary. For example, for canopies like corn where there are

moist vertical stalks, the surface-volume interaction terms are strong in the co-polarized return (Figure 3).

The derivation of analytical expressions for each individual contributing terms depend strongly on the size and distribution of the scatterers (leaves and branches) in the canopy and their relative permittivity. The back scattering coefficients are also dependent on the incidence angle θ and the polarization of the transmit and receive waves. For the polarimetric SAR applications, we only use the co-polarized signals (HH and VV) and the cross-polarized term (HV).

Since we are interested to estimate the canopy water content and the soil moisture, the model is modified to include these variables. We have chosen the canopy water content versus the wet or dry biomass because it is directly computed in the model and it is independent of the type of the vegetation. The co-polarized terms are dependent on both

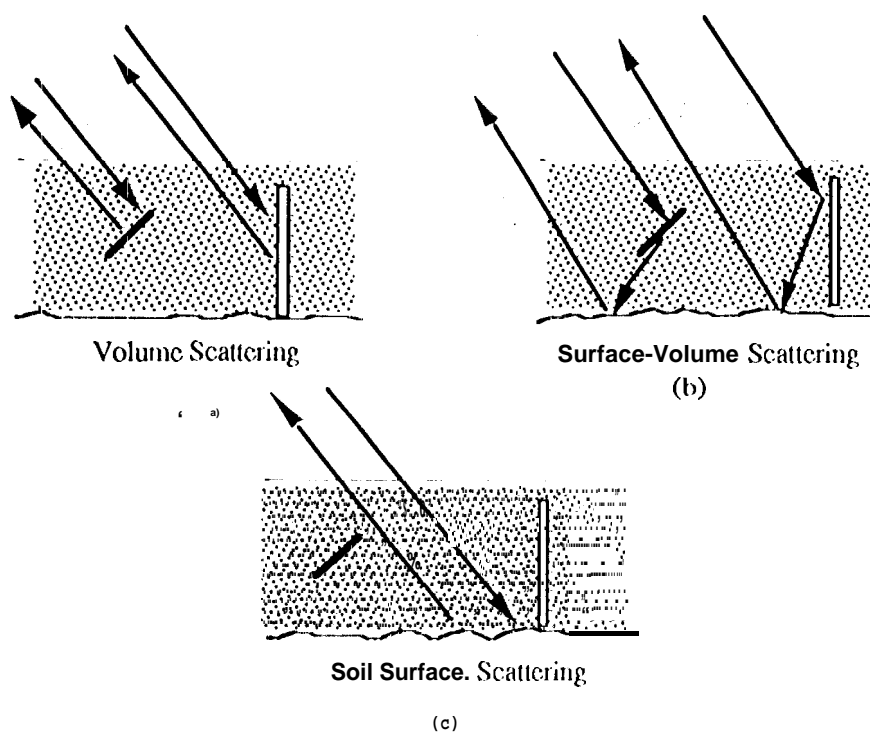


Figure 3. Dominant scattering mechanisms in a vegetation canopy,

canopy and soil parameters. In other words all three independent terms in (1) and (2) are important in simulating the co-polarized return. However, only the volume scattering from the vegetation canopy is important in cross polarized term. The surface scattering and surface volume interaction terms are often negligible when simulating the SAR data over the agricultural fields. It has been shown that the cross polarized term can be written in terms of the canopy water content [Saatchi *et al.*, 1993]. In the next section, we describe the inversion algorithm developed to estimate these parameters from the SAR data.

6.() Inversion Algorithm

6.11 Estimation of Canopy Water Content:

"To estimate the canopy water content we use the fact that the cross polarized return from the SAR data shows a strong correlation with the volume scattering in the vegetation canopy. It has been shown in the previous section that this statement is particularly valid where analyzing the SAR data over the Barrax site at two different dates where the vegetation biomass has changed. Figure 4 shows the HH, VV, and HV SAR returns from irrigated corn fields for both dates of June 19 and July 14. During the June 19 experiment, the corn plants were grown approximately 25 cm and the soil surface was completely exposed. To the radar signal at the L- and C-band this field appears as bare or with very low vegetation. On July 14, the corn plants were grown approximately 1 m high and the soil surface was covered by vegetation. The soil surface was wet and the moisture content remained approximately the same during the two SAR flights. In Figure 4, 100 data points at the same incidence angle, with their mean and standard deviation, extracted from synthesized images over the corn fields are illustrated. The HV term at both frequencies is increased more than 10 dB where the HH and VV terms have shown approximately 5 dB change. As it was mentioned earlier, the cross polarized term is mainly dependent on the Vegetation water content. Whereas, the co-polarized terms are dependent on both vegetation and surface parameters which are difficult to separate. By using the model expression for HV return which has two independent parameters, canopy water content and a frequency independent weighting factor and using the L-band and C-band HV returns from the SAR data, we estimate the canopy water content [Saatchi, 1993]. This algorithm assumes that the canopy water content does not exceed 4 kg/m². Furthermore, for very low values of HV returns, it is assumed that the surface is nonvegetated. Other tests, such as the unsupervised classification, to distinguish between vegetated and nonvegetated areas are also used to guarantee the accuracy of the inversion algorithm [Van Zyl, 1988].

Figure 5 shows the result of the inversion algorithm for the canopy water content. A gray scale has been used to illustrate the result in an image form. The bright circular areas are mainly canopies with high value of water content. Comparison of June 19 and July 14 images show the difference in the state of the canopies and a simple visual way of detecting the changes in the vegetation growth. The results are in agreement with the field observations during the experiment. In other words all the vegetated areas picked by the algorithm match qualitatively with the amount of vegetation in the fields. Due to lack of ground truth data available at this time, the quantitative comparison has been made only over one corn field. Figure 6 shows the comparison between the vegetation water content estimated by the algorithm and the ground truth wet biomass data collected over the field B1. Note that the error is partially due to the fact that we are comparing the water content with the biomass data. By using the appropriate factor to translate the canopy water content to the wet biomass of corn crop, the magnitude of the error may change slightly.

6.2 Soil Moisture Estimation:

It has been shown that the soil surface roughness and the vegetation have significant effect on estimating the soil moisture [Ulaby *et al.*, 1986]. According to equation (1), σ_{soil}^o and $\sigma_{surf-veg}^o$ include the underlying soil parameters such as roughness and dielectric constant (moisture). In the model these terms are expressed in a rough surface scattering model and the DBA formulation. Both terms also depend on the vegetation water content through an attenuation factor. By knowing the canopy water

Content, the effect of the vegetation in the co-polarized terms can be corrected. This correction is readily done by calculating the volume scattering terms and the vegetation attenuation factors in the surface-volume interaction term and the soil backscattering terms. By subtracting the volume scattering term from the total backscattering coefficient, an expression can be found which only depends on the surface dielectric constant and roughness parameters. There are many rough surface scattering models in the literature which can be used to model the corrected backscattering coefficient. In this study, we have used a simple linear model to represent the effect of the surface moisture. This linear equation is obtained by model simulations and the *Least-Squared* fit of the model to the SAR data by adjusting the roughness parameters over known bare fields. The linear equation can be expressed as follows:

$$\sigma_{\text{corrected}}^{\text{olll}} = A(\theta) + B(\theta)M_v \quad (3)$$

where $\sigma_{\text{corrected}}^{\text{olll}}$ is the corrected IIII polarized backscattering coefficient, M_v is the soil moisture and the coefficients $A(\theta)$ and $B(\theta)$ are linear functions of $\cos\theta$ which are found as a result of an optimization technique. The functions $A(\theta)$ and $B(\theta)$ also depend on the frequency. In this study, we use the IIII polarized data at L-band to estimate the soil moisture. At this frequency, the function $B(\theta)$ can be approximated by a constant. Similar approach was used by Ulaby *et al.*, [1982] at C-band. In the above formulation, the incidence angle θ is known for each pixel from the SAR images. By knowing the coefficients of equation (3) one can readily estimate the soil moisture from the SAR images over bare and the vegetated fields.

Figure 7 shows the SAR derived soil moisture images over the Barrax site. A qualitative comparison of the images in Figure 7 with the field observations shows a good agreement. To check the results quantitatively, we have used the soil moisture content from the top 5 cm layer of a dry bare field and an irrigated corn field with very low vegetation (Table 3) to compare with the SAR derived soil moisture in Figure 8. The results illustrate that the algorithm detects the dry and wet fields correctly. However, the absolute values of soil moisture are off by 30%. Furthermore, both images in Figure 7 show that soil moisture values of near range are higher than the far range. This is mainly due to the fact that most of the irrigated fields are in the near range. However, there is an error due to the radar look angle variations since the regression line used in equation (3) does not compensate for the roughness and incidence angle correctly. A rough surface backscattering inversion model in conjunction with SAR polarimetric data may provide better results.

7.0 Summary

In this study, we have used a physically based backscattering model (1111A) to interpret the SAR data and to develop inversion algorithms. Two parameters which are useful in hydrological studies and land-surface atmospheric interaction models are chosen for the retrieval algorithms: the canopy water content, and the surface soil moisture. The IIV backscattering coefficients obtained from the SAR data have shown a strong correlation with the canopy water content. This term is then modeled as to include only the volume scattering contribution. An algorithm using the L- and C-band IIV polarized SAR data was used to estimate canopy water content. The result of the inversion algorithm has shown a good agreement with the ground truth data,

Next, we used the estimated canopy water content in the expression for 1111 polarized backscattered power to correct for the vegetation effects. The corrected 1111 SAR image at 1.-band depends only on the surface moisture. A regression algorithm which relates the SAR data to soil moisture was then used to obtain a new image for soil moisture. The estimated soil moisture over the Barrax site identifies the wet and dry fields accurately but when compared with ground truth data the *rms* error is approximately 30%. The estimation errors in both algorithms are caused by a variety of sources such as the data calibration, modeling approach, and the ground truth measurements. The inversion algorithms can be improved by eliminating or reducing the sources of errors.

REFERENCES

- Bolle, J. J., Streckenbach, B., "The ECIVAI. Field Experiment in a Desertification-Threatened Area (EFIDA): First Annual Report," Free University of Berlin, FRG, 1992.
- Dobson, M. C., Ulaby, F. T., LeToan, T., Beaudoin, A., Kasischke, J. S., and Christensen, N., "Dependence of Radar Backscatter on Coniferous Forest Biomass," *IEEE Trans. Geoscience Remote Sensing*, Vol. 30, pp. 412-415, 1992.
- Engman, E. T. and Gurney, R. J., *Remote Sensing in Hydrology*, Chapman and Hall, London, United Kingdom, 1991.
- Evans, D. L. and Van Zyl, J. J., "Imaging radar polarimetry: analysis tools and applications," Chapter 7 in *PIERS-3 Polarimetric Remote Sensing*, J. A. Kong (Ed), Elsevier, New York, 1990.
- Lang, R. H. and Sidhu, J. S., "Electromagnetic backscattering from a layer of vegetation: a discrete approach," *IEEE Trans., GRS*, GI-21: 62-71, 1983.
- LeToan, T., Beaudoin, A., Riou, J., and Guyon, D., "Relating forest biomass to SAR data," *IEEE Trans. Geoscience Remote Sensing*, Vol. 30, pp. 403-411, 1992.
- Saatchi, S. S., Lang, R. H., and LeVine, D. M., "Microwave backscattering and emission model for grass canopies," in press, *IEEE Trans. Geoscience Remote Sensing*, 1993.
- Saatchi, S. S., "Estimation of canopy water content from SAR imagery," to be submitted to *IEEE Trans. Geoscience Remote Sensing*, 1993.
- Ulaby, F. T., Moore, R. K., and Fung, A. K., *Microwave Remote Sensing: Active and Passive*, Vol. II - *Volume Scattering and Emission Theory, Advanced Systems and Applications*, Artech House, Dedham, Massachusetts, 1986.
- Van Zyl, J., "Unsupervised classification of scattering behavior using polarimetry data," *IEEE Trans. GRS*, GI-27:36-45, 1989.
- Van Zyl, J., Chapman, B., Dubois, P., and Freeman, A., "TOI. CA]. user's manual: Version 4.0 Upgrade," JPL 11-7715, Jet Propulsion Laboratory, 1992.
- Vissers, M. A. M. and Hockman, D. H., "Soil data collection for the JPL-SAR campaign during EFIDA," Preliminary Report, Wageningen Agricultural University, Dept. of Hydrology, The Netherlands, 1992.

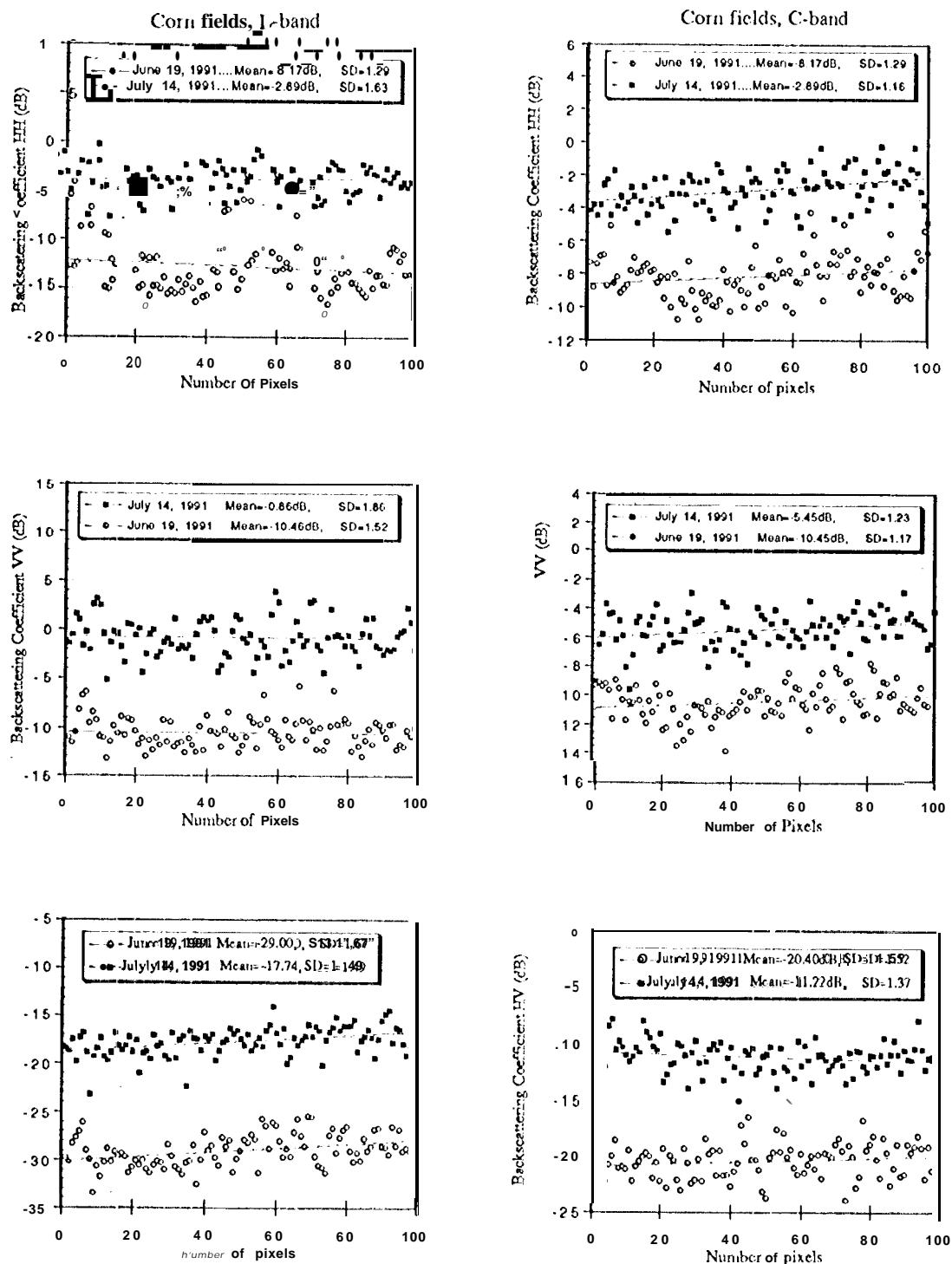


Figure 4. Comparison of co-polarized anti cross-polarized returns at L-band and C-band from an irrigated corn field.

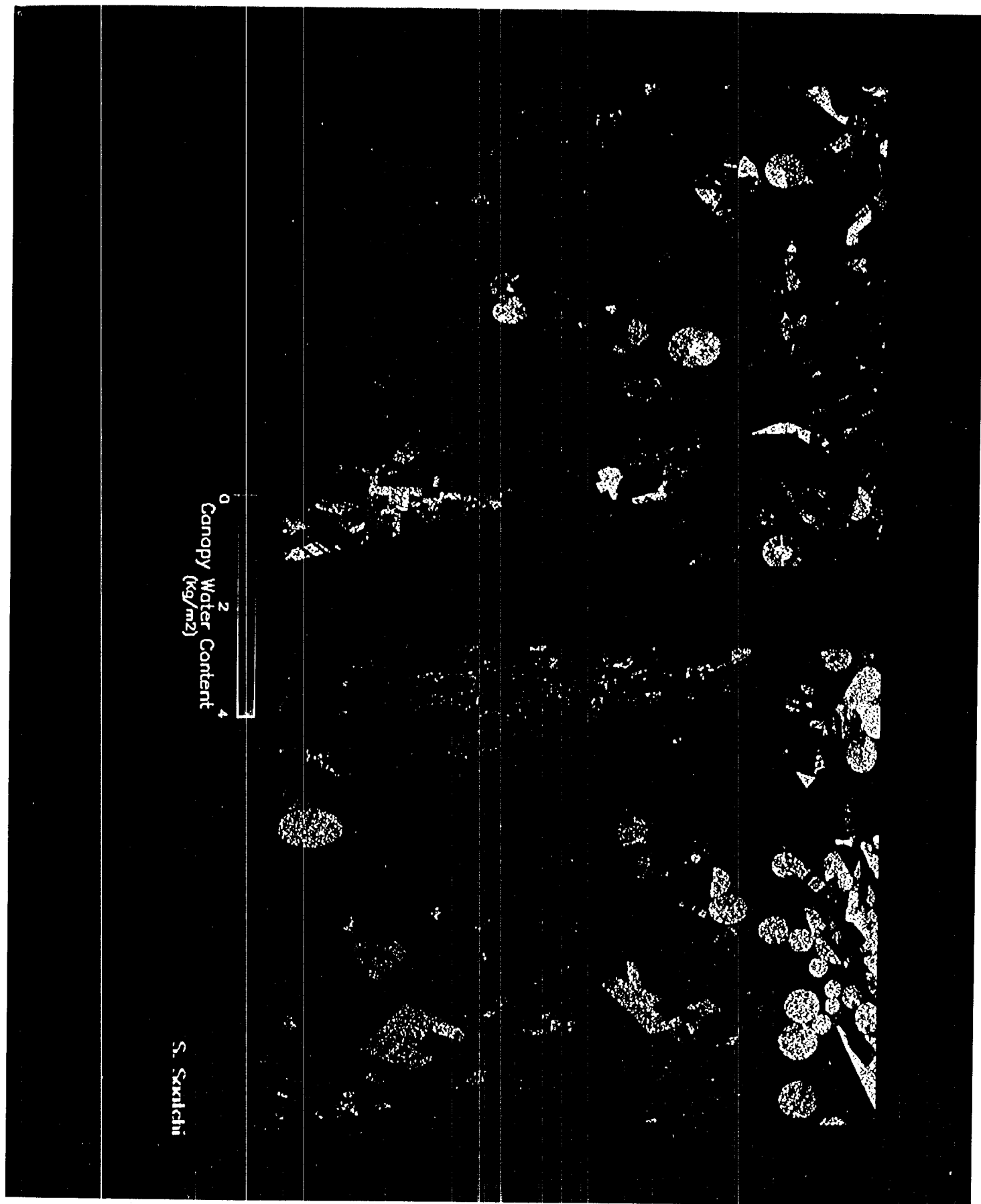


Figure 5. SAR derived canopy water content over Barrax site for June 19 (left) and July 14 (right) data sets.

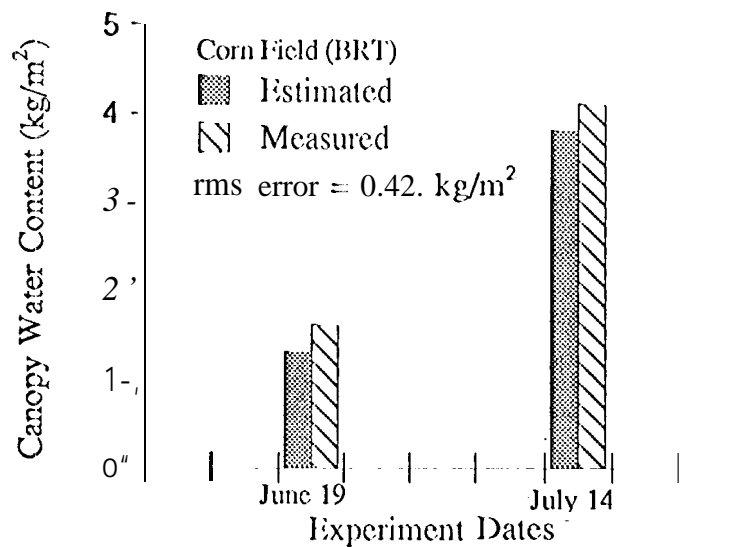


Figure 6. Comparison of estimated and measured canopy water content over a corn field in Barrax site.

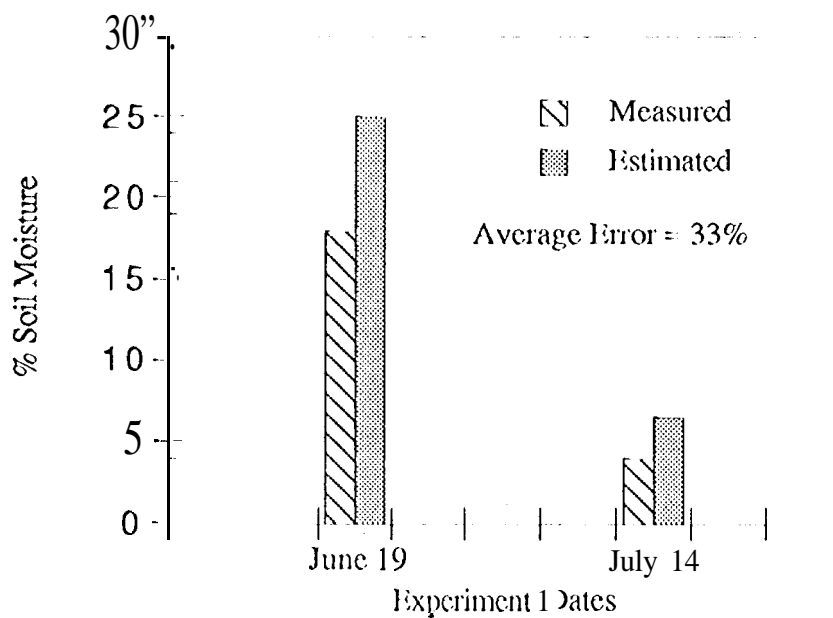


Figure 8. Comparison of measured and estimated soil moisture of a dry and wet field over Barrax site.

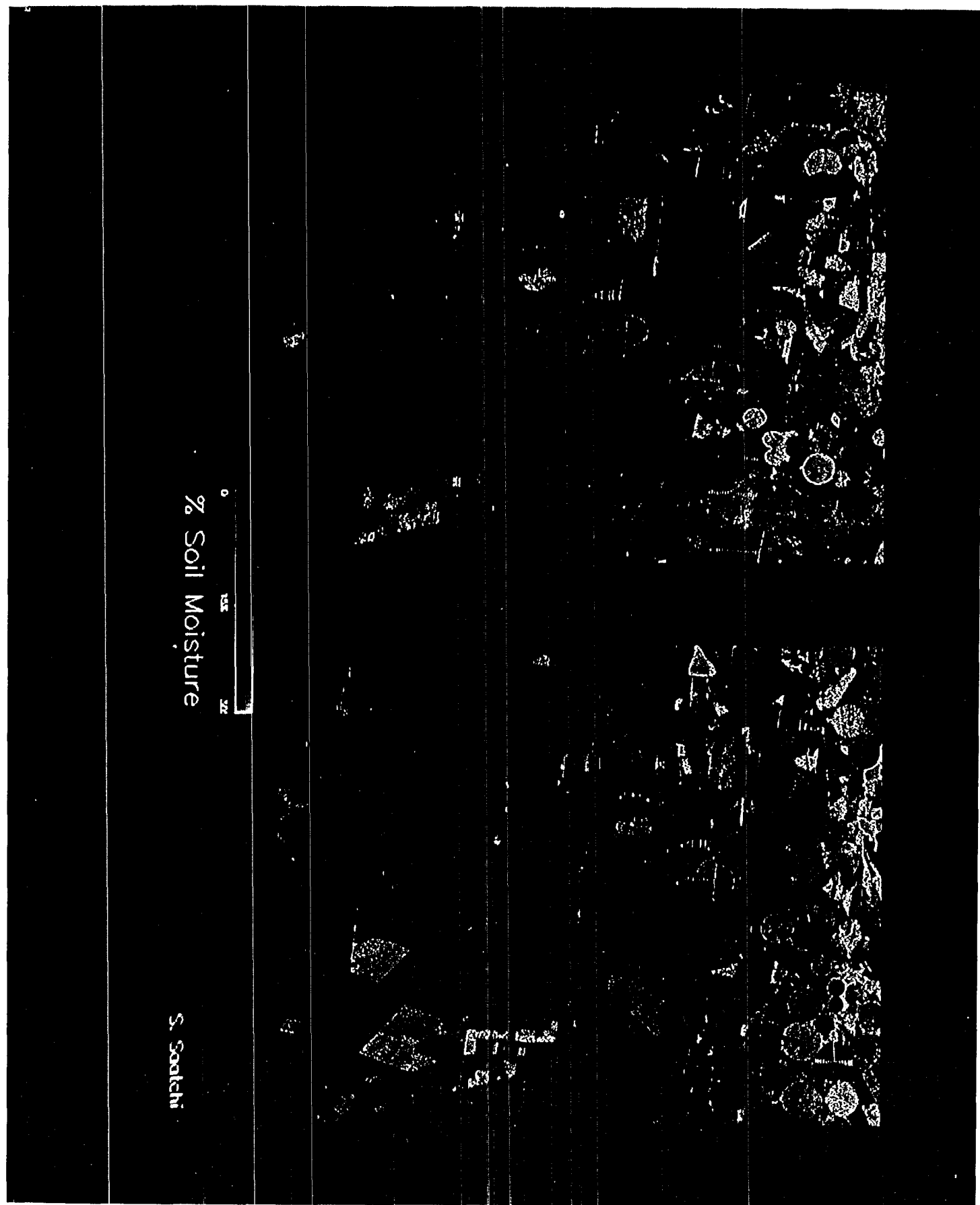


Figure 7. SAR derived soil moisture over Barrax site for June 19 (left) and July 14 (right) data sets.